European Polymer Journal 69 (2015) 403–415

Contents lists available at ScienceDirect

European Polymer Journal

journal homepage: www.elsevier.com/locate/europolj

Rosin based epoxy coating: Synthesis, identification and characterization

Rasha A. El-Ghazawy *, Ashraf M. El-Saeed, H.I. Al-Shafey, Abdul-Raheim M. Abdul-Raheim, Maher A. El-Sockary

Egyptian Petroleum Research Institute, Nasr City, 11727 Cairo, Egypt

ARTICLE INFO

Article history:
Received 18 September 2014
Received in revised form 6 June 2015
Accepted 19 June 2015
Available online 20 June 2015

Keywords:
Rosin
Diels–Alder adduct
Epoxy coating
Liquid crystal curative
Thermal stability

ABSTRACT

Ketone type derivative of rosin was prepared by dehydrocarboxylation of isomerized abietic acid. Coupling of dipimaryl ketone with maleic anhydride was performed by acetic acid catalyzed Diels–Alder reaction. Afterwards, the dipimaryl ketone was epoxidized to get the corresponding tetra glycidyl ester. The chemical structure of the synthesized products was confirmed by UV, FTIR and ^{1}H NMR spectroscopic analyses. Cured resins using a rosin-based crosslinker and p-phenylene diamine (a commercial crosslinker) were evaluated using dynamic mechanical analysis (DMA), thermogravimetric analysis (TGA) and some preliminary universal coating tests. Results showed that the fully rosin-based epoxy system gave better performance than commercially bisphenol-A based one. This finding was attributed to a liquid crystal behavior of the rosin-based crosslinker. Mesomorphic transition temperature and liquid crystalline texture of the rosin-based crosslinker were investigated by polarized optical microscopy (POM) and differential scanning calorimetry (DSC).

1. Introduction

The increasing demand to maximize bio-based share in various products is now a challenging target. Rosin obtained from exudate of pine and fir trees with annual world-wide production of about 1.27 million tons contains abietic acid as a major component. Low cost, availability and derivatization ability [1] widen application of the latter in many fields. This diterpene acid contains hydrophenanthrene moiety with two conjugated double bonds besides its reactive carboxylic group. Rosin was used in modifying phenol–formaldehyde resins through Diels–Alder cycloaddition of resole to infer oil solubility for surface coating application [2]. The hydrophenanthrene moiety provides resin acids with hydrophobicity, a property that facilitated their use in marine antifouling coating materials for decades [3]. It also found application in printing inks through modification with formaldehyde resins [4,5] and polyester of phthalic anhydride and glycerol [6]. Recently, rosin-based compounds were used as a novel one component i-line molecular glass photoresists [7]. Moreover, a great interest was observed in preparing rosin based polymers for enhanced thermal stability [8,9] as well as polyesters [10,11], epoxy resins [12–15] and epoxy curatives [16–20].

The objective of this research was directed to make use of the rigidity of the tricyclic hydrophenanthrene structure of rosin acids in order to prepare a fully bio-based two component epoxy coating epoxy resin and crosslinker – with enhanced

* Corresponding author.
E-mail address: basharosh_00@yahoo.com (R.A. El-Ghazawy).

http://dx.doi.org/10.1016/j.eurpolymj.2015.06.025
0014-3057/

performance. In this context, tetraglycidyl dimaleopimaryl ketone (epoxy resin) was prepared and cured with either a rosin acid based crosslinker (RC) or the traditional p-phenylene diamine crosslinker (PPD) for comparison.

2. Experimental

2.1. Materials

Abietic acid (75%) was obtained from Sigma–Aldrich. It is indeed a mixture of rosin acids with abietane type as a main component (75%) where most of the neutral compounds are distilled off [17]. Maleic anhydride (⩾99%), p-toluene sulfonic acid monohydrate (⩾98.5%), 1,1′-(methylenedi-4,1-phenylene) bismalimide (95%) and epichlorohydrin (99%) were purchased from Sigma–Aldrich. Sodium hydride suspension (60% in paraffin oil) was obtained from Loba Chemie chemical company – India and p-phenylene diamine (97%) was obtained from Central Drug House chemical company – India. Acetic acid (99.5%), dimethyl formamide (99.8%) and zinc acetate dihydrate (97+%) were delivered from Acros Organics chemical company – Belguim. 2-ethyl-4-methylimidazole (96%) was purchased from Alfa-Aesar chemical company – USA. A commercial diglycidylether bisphenol-A (DGEBA) sample under the trade name of KEMAPOXY150 was kindly supplied by Chemicals for Modern Building Company (CMB) – Egypt (having epoxy equivalent weight of 182–192 g/mol). All chemicals were used as received without further purification.

2.2. Measurements and characterization

^{1}H NMR spectra were recorded on Varian NMR 300 MHz spectrometer in deuterated chloroform. FTIR spectra were measured on a Mattson-infinity series bench top 961 spectrometer. UV spectra were recorded on Shimadzu UV-1600 series. Elemental analyses were performed on Shimadzu Qp-2010 plus while total acid number was evaluated according to ASTM D-664 on MATi 02 Automated TAN/TBN analysis, Metrohm. Epoxy equivalent weight was experimentaly investigated according to ASTM D-1652 and calculated using ^{1}H NMR analysis data [21]. DMA was carried out on Triton Technology DMA using a three point bending mode. Samples were tested from 30 to 200 °C at a heating rate of 10 °C min^{-1} and frequency of 1 Hz. Thermogravimetric analysis was conducted using Simultaneous DSC–TGA, Q 600 SDT thermogravimetric analyzer. Microscopic observations were investigated using Olympus polarizing microscope (POM) at a magnification of 100 with crossed polarizers. For mechanical, chemical and corrosion analyses of cured epoxy resins, coat samples were mixed and applied with a total dry film thickness (DFT) of 100 μm. As commonly used, mild steel panels (15 cm × l0 cm) were used to evaluate different properties of the coatings. The other side of the panels was coated and protected against corrosive environments by using coal tar epoxy primer. The tested side was blasted and cleaned before coating. The panels were then subjected to different testing procedures for evaluating their mechanical properties and their durability. Mechanical assessments of the coated steel samples including impact resistance and pull-off resistance were evaluated according to ASTM D5420 and ASTM D4541, respectively, while hardness and bending tests were examined using ASD 3363 and D522, respectively.

2.3. Synthesis of tetraglycidyl dimaleopimaryl ketone (TGK)

Synthesis route of tetraglycidyl dimaleopimaryl ketone is presented in Scheme 1. Isomerization of 30.2 g (0.1 mol) abietic acid into levopimaric acid was performed under a continuous stream of nitrogen and carbon dioxide at 180 °C for four hours [16,18,22]. Isomerization was followed up using UV spectroscopy. Dipimaryl ketone was synthesized according to a procedure reported by Bicu and Mustata [23]. Maleodipimalryl ketone was prepared following Diels–Alder cycloaddition protocol using 0.7 g zinc acetate as catalyst and acetic acid as a solvent. After 12 h of reflux a brownish yellow solid was collected. A yield of 85% was obtained after double recrystallization from acetic acid then washed with water. A mixture of maleodipimalryl ketone 21.3 g (0.021 mol) in dimethyl formamide (DMF), purified sodium hydride 1.27 g (0.052 mol) and epichlorohydrin 78.51 ml (0.84 mol) was placed in a three-neck flask and refluxed for 6 h. An extra amount of sodium hydride was added by the end of the reaction. After getting rid of the solid precipitate, the excess of epichlorohydrin and the solvent was evaporated under vacuum. The final product was washed using methanol two times and dried under vacuum at 40 °C. The chemical structure of dipimaryl ketone, maleodipimalryl ketone and tetraglycidyl dimaleopimaryl ketone was confirmed using elemental analysis, melting point (T_m), total acid number (TAN), FTIR and ^{1}H NMR.

2.4. Preparation of a rosin-based crosslinker (RC)

RC was prepared and purified according to a procedure described by Liu and coworkers [16]. Synthesis route of the rosin-based crosslinker is presented in Scheme 2. Thermal transitions of RC were identified by DSC where the sample was heated from room temperature up to 350 °C with a heating rate of 10 °C/min under nitrogen atmosphere. In addition, POM was used to determine the texture during a heating regime.

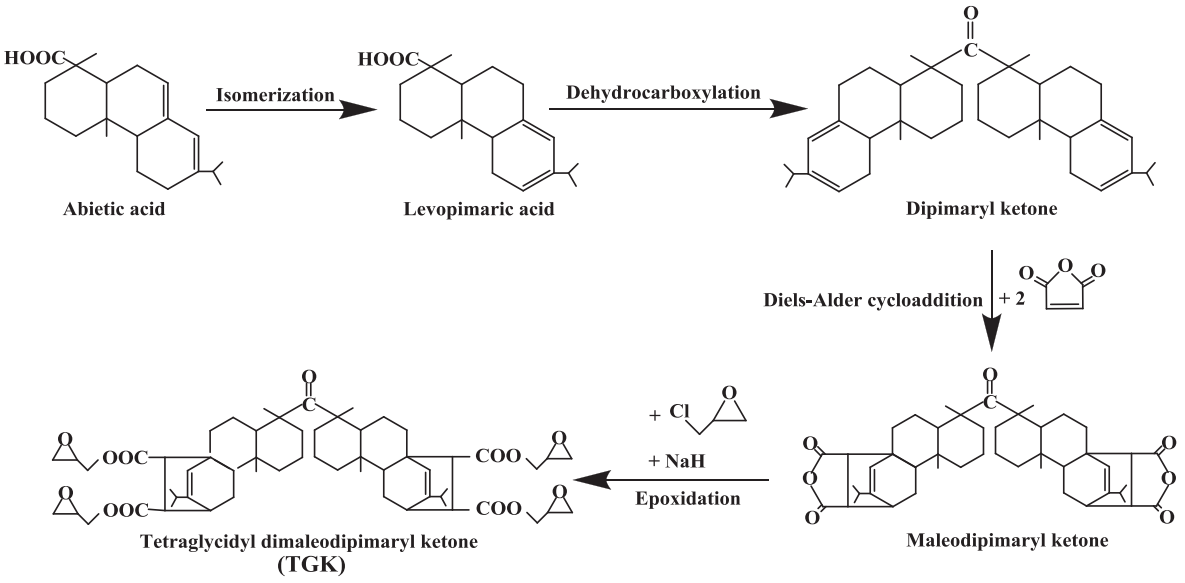

Scheme 1. Synthetic route for TGK.

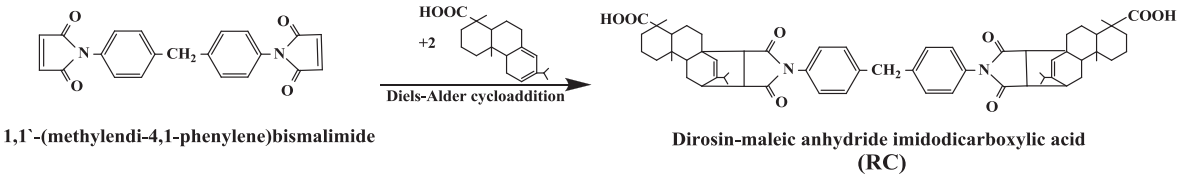

Scheme 2. Synthetic route for RC.

2.5. Epoxy curing

The tetraglycidyl dimaleopimaryl ketone (TGK) was cured using the rosin-based crosslinker (RC) with stoichometric amounts and the aid of 1 wt% 2-ethyl-4-methylimidazole as an accelerator. After good mixing using DMF, the solvent was evaporated under vacuum then the mixture was poured into low surface energy molds with dimensions: 60 mm × 5 mm × 2 mm. Curing was achieved at 120 °C for 2 h. The cured sample was left to cool at room temperature before demolding for DMA analysis. The thermal stability of the cured resins was also evaluated using TGA. The same procedures for curing were followed using TGK/PPD (p-phenylene diamine) and DGEBA/PPD.

3. Results and discussion

Gum rosin contains about 90% abietic acid and its isomers in addition to other neutral components. Two main types of functional groups can be utilized in abietic acid: heteroannular conjugated double bonds and carboxylic acid groups. Knowing that levopimaric acid (with homoannular double bonds) is the only isomer that can undergo Diels–Alder cycloaddition, abietic acid was first isomerized to pimaric form at high temperature. Dehydrocarboxylation of levopimaric acid leads to bisdiene that can be chemically modified through Diels–Alder protocol to get dimaleopimaryl ketone. The latter is a good candidate for preparing tetrafunctional epoxy resins. Considering that the increase in functionality of either the epoxy resin or its crosslinker may result in more condensed crosslinked network, we prepared tetraglycidyl ester of rosin-based epoxy which may lead to favorable rigidity. Optimizing the stoichiometric amount of hardener and its type would provide epoxies with improved mechanical and thermal properties. In this study, a rosin-based crosslinker (previously prepared by Liu and coworkers [16]) and a commercially available crosslinker (p-phenylene diamine (PPD)) were used to investigate the possibility of introducing a fully bio-based epoxy system.

3.1. Synthesis and characterization

The synthesis scheme of the tetraglycidyl dimaleopimaryl ketone (TGK) is shown in Scheme 1. Elemental analyses, melting point (T_m) and total acid number (TAN) of abietic acid, levopimaric acid, dipimaryl ketone, maleodipimalryl ketone and TGK data are presented in Table 1. The isomerization of abietic acid to levopimaric acid is asscociated with a slight change in

TAN. FTIR spectrum of levopimaric acid (Fig. 1) shows a characteristic band at 1693.19 cm^{-1} for the carboxylic acid C=O group. The formation of levopimaric acid with its characteristic homoannular double bonds was sucessfuly confirmed by UV spectroscopy. Levopimaric acid shows an absorption at λ_{max} 247 nm (Fig. 2a) indicating efficient isomerization into pimaric structure whereas abietic acid absorption can be observed at λ_{max} 233 and 240 nm (Fig. 2b).

In the dehydrocarboxylation step, the low melting point of dipimaryl ketone (90 °C) with respect to levopimaric acid (158 °C) (Table 1) in addition to the decreased TAN value of the former (15.63) to about half that of levopimaric acid (184.37) proofs participation of carboxylic acid groups in ketone formation. FTIR spectrum of the dipimaryl ketone is shown in Fig. 1. A diminished OH absorption band at 3402.89 cm^{-1} and a strong ketonic C=O absorption band at 1772.87 cm^{-1} can be observed. These results gave a further indication for the efficient involvement of carboxylic acid groups in the dehydrocarboxylation reaction.

Different catalysts including hydroquinone, phosphoric acid and p-toluene sulfonic acid with acetic acid were used in Diels–Alder cycloaddition of maleic anhydride into isomerized rosin acids [16–18,20,24]. Through surveying literature, it was found that using phosphoric acid as a catalyst in Diels–Alder reaction gave a low yield (54%) while hydroquinone induced better yield (66%) and p-toluene sulfonic acid with acetic acid resulted in the best yield (92%). For that reason, p-toluene sulfonic acid with acetic acid was selected for Diels–Alder cycloaddition.

The chemical structure of maleodipimalryl ketone was confirmed by FTIR and ^{1}H NMR. The FTIR spectrum (Fig. 3a) shows the appearance of 1777.08 cm^{-1} and 1847.47 cm^{-1} characteristic signals for C=O stretch of maleic anhydride. The ^{1}H NMR spectrum (Fig. 4) shows a peak at 5.30 ppm attributed to protons *a* that are attached to the unsaturated carbon formed after Diels–Alder adduction. A multiplet peak at 2.95 ppm assigned to protons *b* of succinic anhydride and another one at 2.36 ppm assigned to protons *c*, can be observed. The characteristic peak assigned to COOH proton in the range of 10–12 ppm cannot be observed. This verifies the consumption of pimaryl carboxylic acid group in ketone formation while keeping anhydride ring without hydrolysis.

In FTIR of TGK (Fig. 3b), the new formed ester carbonyl groups show absorption band at 1728.87 cm^{-1} while the epoxide ring gives three bands for C–O stretching vibration; symmetric stretching at 1242.90 cm^{-1} and asymmetric stretching at 823.45 cm^{-1} and 751.14 cm^{-1}. Disappearance of maleic anhydride symmetric and asymmetric C=O stretching vibrations (at 1847.47 cm^{-1} and 1777.08 cm^{-1}) can also be observed. Fig. 5 shows ^{1}H NMR spectrum of TGK. The peak at 5.34 ppm is assigned to the double bond protons (*a*). The terminal glycidyl groups were characterized by the peaks found at 4.20 ppm and 3.62 ppm for methylene protons *b* and *c*, respectively. The peak observed at 3.3 ppm is assigned to protons *d* while the peaks that appear at 2.90 ppm are attributed to protons *e* and *f*.

The equivalent epoxy weight (EEW) for TGK was determined according to ASTM D-1652 giving an EEW of 285 g/eq. This value was used for calculating the suitable amount of crosslinker required for curing reaction. The value of EEW was also calculated using ^{1}H NMR analysis [21]. The functionality of the epoxy was calculated [25] by relating the integration of the two double bond protons (peak "a" of Fig. 5) to that of the epoxy protons attached to the more substituted carbon (peak "d" of Fig. 5). Therefore, the functionality of the epoxy is given by $(1.01/0.61) \times 2/1 = 3.31$. The EEW is then calculated by relating the theoretical molar mass of the epoxy to its functionality [21]: $EEW = [771 + (3.31 \times 57.07)]/3.31 = 290$ g/eq. It can be noticed that although both EEW values – determined by ASTM and by ^{1}H NMR – are in good agreement but they are higher than the theoretical one (EEW = 250). This observation may be attributed to anomalous condensation reaction, incomplete dehydrohalogenation reaction and/or the impurity of the starting abietic acid (purity = 75%) that also contains different resin acids susceptible to epichlorohydrin condensation.

In this context, the percentage of opened epoxy groups was calculated using ^{1}H NMR analysis data [21]. The employed methodology is based on calculating the integration of the protons assigned to the opened epoxy groups (five protons: *b′*, *c′*, *d′*, *e′* and *f′*) as a measure of the latter ratio. These protons are observed between 3.5 and 4.8 ppm (Fig. 5). The integration corresponding to this region includes the contribution of protons *b* and *c* belonging to the closed epoxy rings as well. Thus, the ratio of the opened epoxy groups can be given as the difference between the total integration of the region 3.5–4.8 ppm and the integration of protons *b* and *c* i.e. double the integration of protons *d* (i.e. the ratio of opened epoxy groups = $3.24 - (2 \times 1.01) = 1.22$). Assuming the respective content of opened and closed epoxy rings as *X* and *Y*, thus $5X/1Y = 1.22/1.01$ and $X + Y = 1$. Finally, we get $X = 0.2$ and $Y = 0.8$ that corresponds to 20% opened epoxy groups and 80% closed epoxy groups.

Table 1
Elemental analysis, total acid number (TAN), melting point (T_m) and epoxy equivalent weight (EEW) data for Scheme 1 products and RC.

Sample	C%		H%		N%		TAN (mg KOH g^{-1})		EEW (g/mol)	T_m (°C)
	Calc.	Exp.	Calc.	Exp.	Calc.	Exp.	Calc.	Exp.		
Abietic acid	79.4	78.54	9.9	7.47	–	–	185.7	183.98	–	160
Levopimaric acid	79.4	79.71	9.9	6.54	–	–	185.7	184.37	–	158
Dipimaryl ketone	86.3	85.55	10.7	10.31	–	–	0	15.63	–	90
Dimaleopimaryl ketone	77.9	76.79	7.1	6.53	–	–	297.6	327.4	–	105
TGK	72.1	71.87	7.3	6.74	–	–	0	5.3	285[a], 290[b]	–
RC	76.1	74.24	7.7	7.26	2.9	2.87	116.3	112.65	–	300

[a] EEW value calculated using ASTM D-1652.
[b] EEW calculated using ^{1}H NMR analysis data (theoretical EEW = 250).

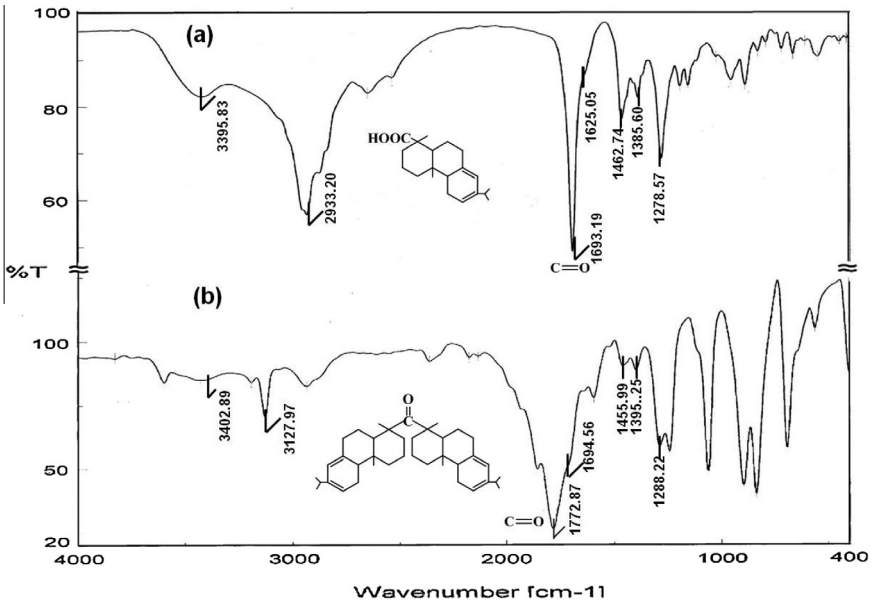

Fig. 1. FTIR spectra for: (a) levopimaric acid and (b) dipimaryl ketone.

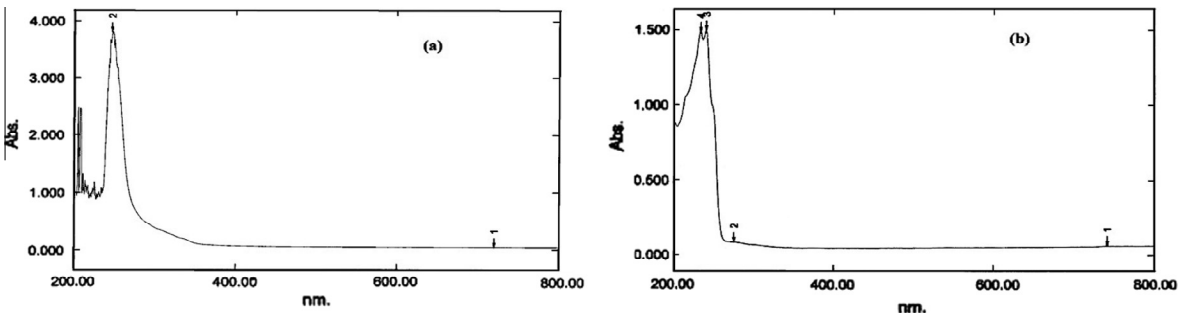

Fig. 2. UV spectrum of (a) levopimaric acid and (b) abietic acid.

The rosin-based crosslinker (RC) was prepared according to Scheme 2. T_m of the RC was recognized at a high temperature (300 °C, see Table 1). This value is higher than that of the starting materials confirming the formation of a new compound. FTIR spectrum of RC (Fig. 6) shows a characteristic band at 3441.35 cm^{-1} assigned to carboxylic acid O—H and intense bands at 1704.76 cm^{-1} and 1838.23 cm^{-1} attributed to C═O groups of carboxylic acid and maleimide moieties. ^1H NMR would be more helpful in confirming the structure of RC (Fig. 7). It shows peaks for the new formed bonds after Diels–Alder cycloaddition including: protons *a* of the new formed unsaturation appears at 5.40 ppm and protons *b* of succinimide observed at 2.91 ppm. In addition, a diminished C—H peak at 6.8 ppm – attributed to double bond of the maleimide reactant – was noticed.

3.2. DMA of cured epoxy systems

The samples were prepared according to dimensions provided by DMA instrument manufacturer for three point bending mode. In Fig. 8, the DMA storage modulus (G') for TGK/RC is compared with TGK/PPD and DGEBA/PPD at different temperatures. Typical storage modulus curves were obtained for the tested samples. It is of interest to mention that, excellent thermal and mechanical properties are likely related to crosslink density, structural order [26] and nature of repeating units. The storage modulus measurements were found to give different stiffness ranking of the tested cured epoxies (TGK/RC > DGEBA/PPD > TGK/PPD). G' values for the cured samples at 25 °C are listed in Table 2. For the TGK cured epoxies, the rigid structure of the RC crosslinker and the possibility of hydrogen bonding, may lead to enhanced mechanical and thermal properties of TGK/RC compared with TGK/PPD. Furthermore, similarity in TGK epoxy structure with that of RC crosslinker may contribute to modulus properties of the cured epoxy. A proposed crosslinked network structure for TGK/RC is shown in Scheme 3. TGK/PPD cured epoxy shows the least storage modulus across the entire tested temperature range. This may be

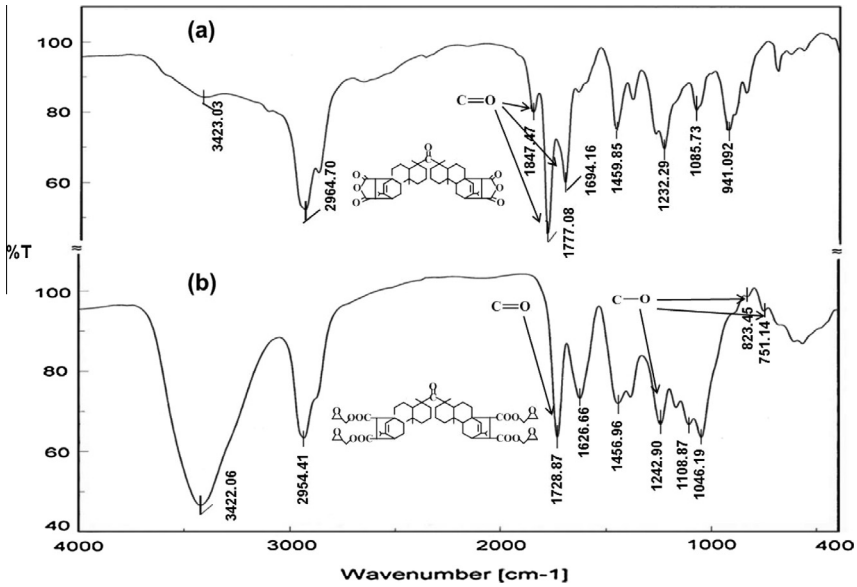

Fig. 3. FTIR spectra for: (a) maleodipimalryl ketone and (b) tetraglycidyl dimaleopimaryl ketone.

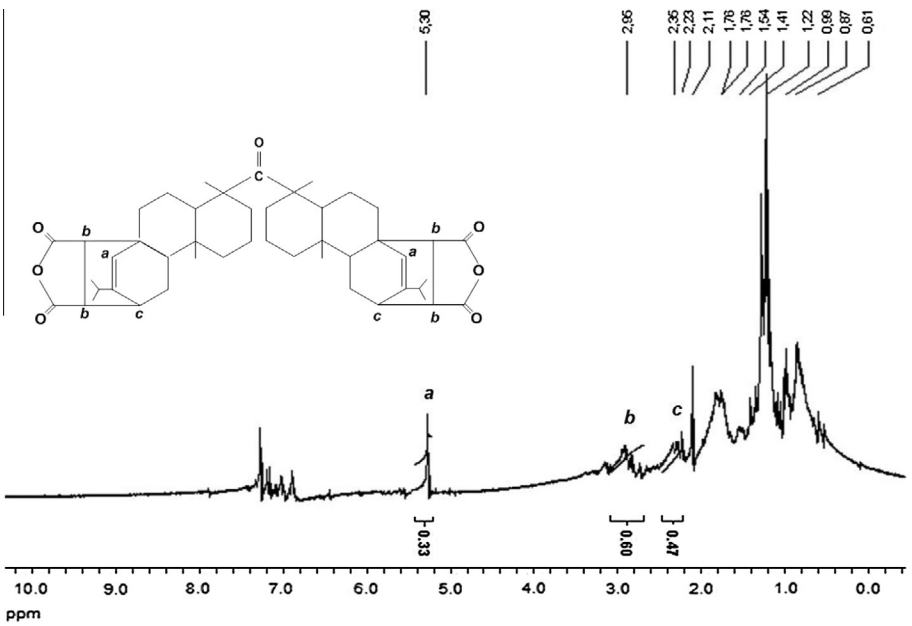

Fig. 4. ^{1}H NMR spectrum of maleodipimalryl ketone.

attributed to the nature of the epoxy components (resin and crosslinker). Resemblance in chemical structure may give room for more interaction and well ordered network structure. Recently in the same framework, Brocas et al. [27] prepared endocyclic epoxidized abietic acid (EAA) and its derivative with pendant epoxy groups (EpAA) as co-precursors for epoxy resins. Cured epoxies of DGEBA/20% EAA or DGEBA/40% EpAA with equivalent amount of isophorone diamine crosslinker (IPDA) show relatively low elastic moduli (4×10^8 Pa and 2×10^8 Pa, respectively). Using the same crosslinker, DGEBA with 20% endocyclic epoxidized Polygral results in a material with approximately half modulus of pristine (1 GPa) [15]. However, standalone exocyclic epoxidized polygrals cured with IPDA show high moduli reaching 0.95 and 1.2 GPa. This signifies the contribution of diterpene acid structure to stiffness as well as the positive role of structural similarity of both resin and hardener.

The increase in temperature leads to a significant decrease in G' for all cured samples. Such decrease is associated with an increase in mechanical loss factor ($\tan\delta$). Peak maximum of $\tan\delta$ versus temperature identifies the glass transition temperature, T_g. The results are summarized in Table 2 where TGK/RC and TGK/PPD show higher T_g than DGEBA/PPD. This may be

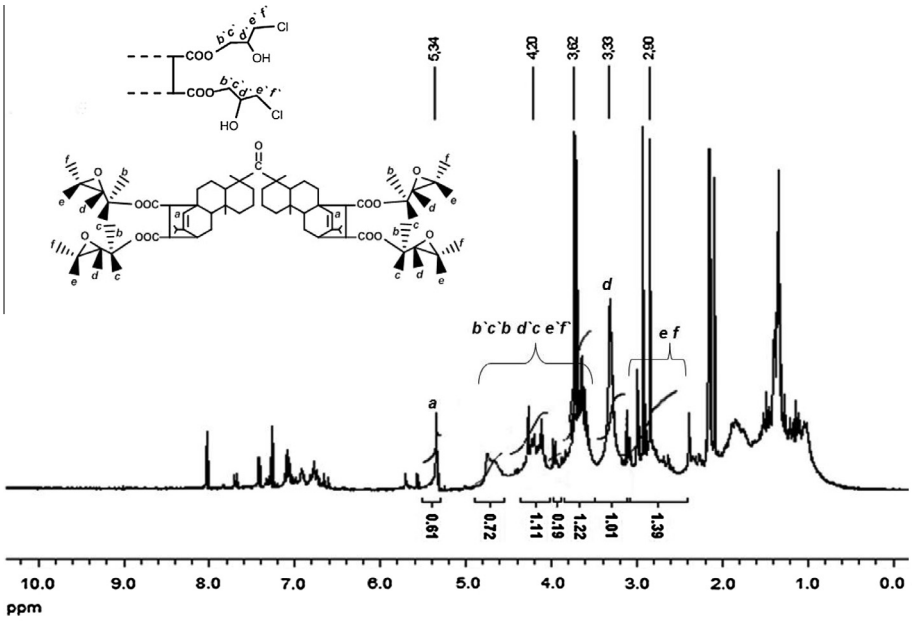

Fig. 5. ^{1}H NMR spectrum of TGK.

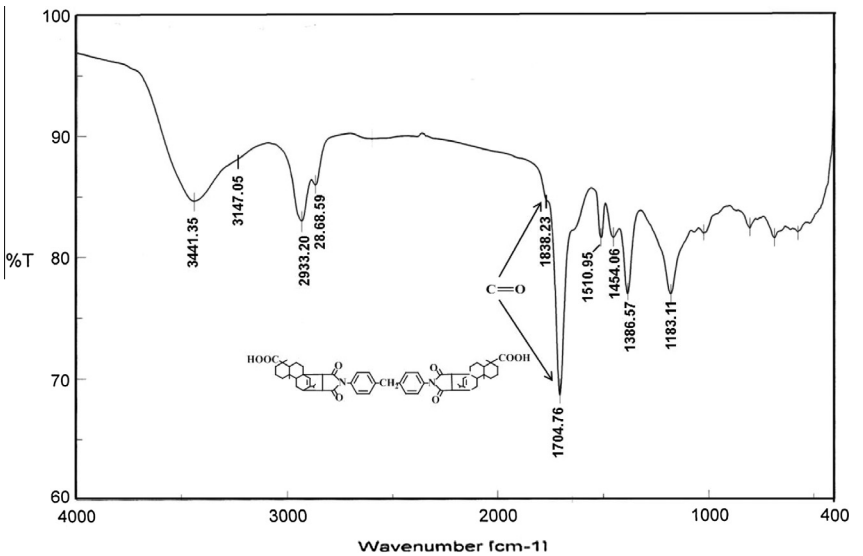

Fig. 6. FTIR of RC.

related to more restricted polymer chains induced by bulky hydrophenanthrene moiety. For RC as a crosslinker, cured epoxies experienced high T_g values (Table 2). This observation also reflects the decrease in segmental mobility and chain mobility as a result of the existence of hydrogen bonds [28,29]. This behavior is in accordance with previously reported data [30–33] where phenyl-based epoxy resins exhibit lower T_g than those of naphthalene-based epoxy resins.

3.3. Thermal stability of cured epoxies

Studying the degradation of thermosetting systems, namely derivatives of epoxy resins, has been an object of constant research [34–37]. The information obtained by the controlled degradation of the polymer can be used to decide whether a given system will be useful for a high temperature application or not. Thermal degradation of all post-cured epoxy systems were evaluated from room temperature to 600 °C under nitrogen atmosphere using a heating rate of 20 °C/min. Thermal stability was investigated with regard to initial decomposition temperature (IDT) and the temperature at which the rate of

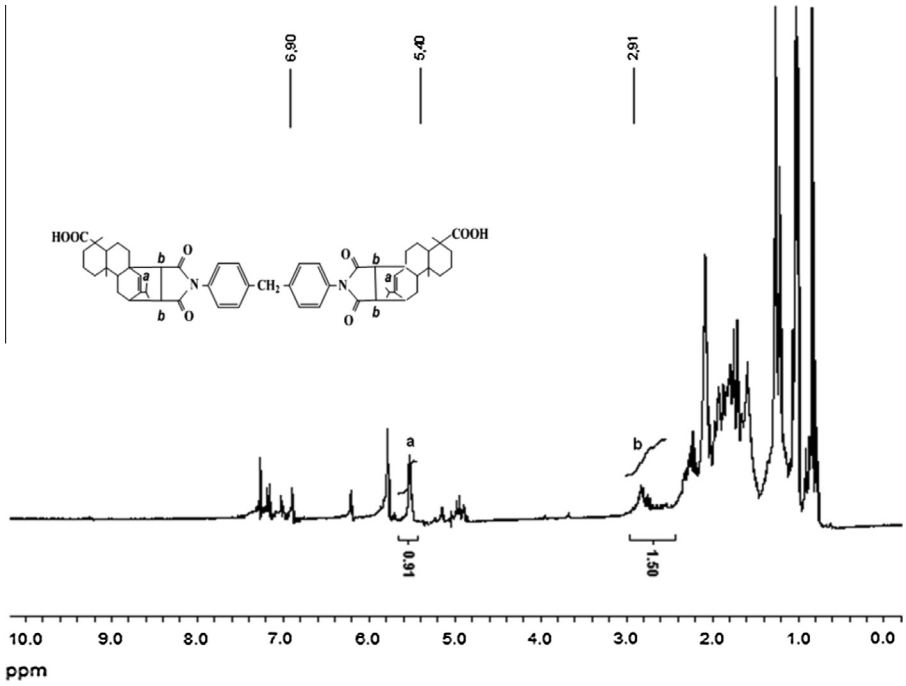

Fig. 7. ^{1}H NMR of RC.

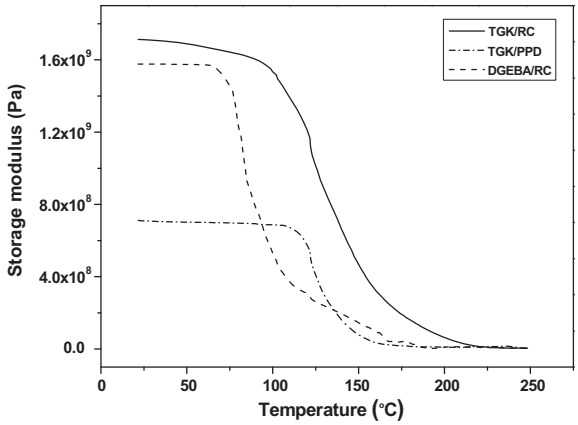

Fig. 8. Plots of storage modulus versus temperature for TGK/RC, TGK/PPD and DGEBA/PPD.

Table 2
Storage modulus (G') at 25 °C and glass transition temperatures (T_g) of cured epoxies.

Sample	G' at 25 °C (GPa)	T_g (°C)
TGK/RC	1.71	140
TGK/PPD	0.71	122
DGEBA/PPD	1.58	90

weight loss obtained from TGA/DTG traces is maximal (T_{max}). Figs. 9 and 10 present TGA/DTG traces of TGK/RC and TGK/PPD showing multiple decomposition stages while TGA/DTG traces of DGEBA/PPD (Fig. 11) have two stages. The first stage of weight loss is generally due to the release of moisture while the following stages indicate the decomposition of the polymer. For TGK/RC, IDT starts at 361 °C and T_{max} is 389.39 °C for the first stage. In the case of PPD cured epoxies, i.e. samples

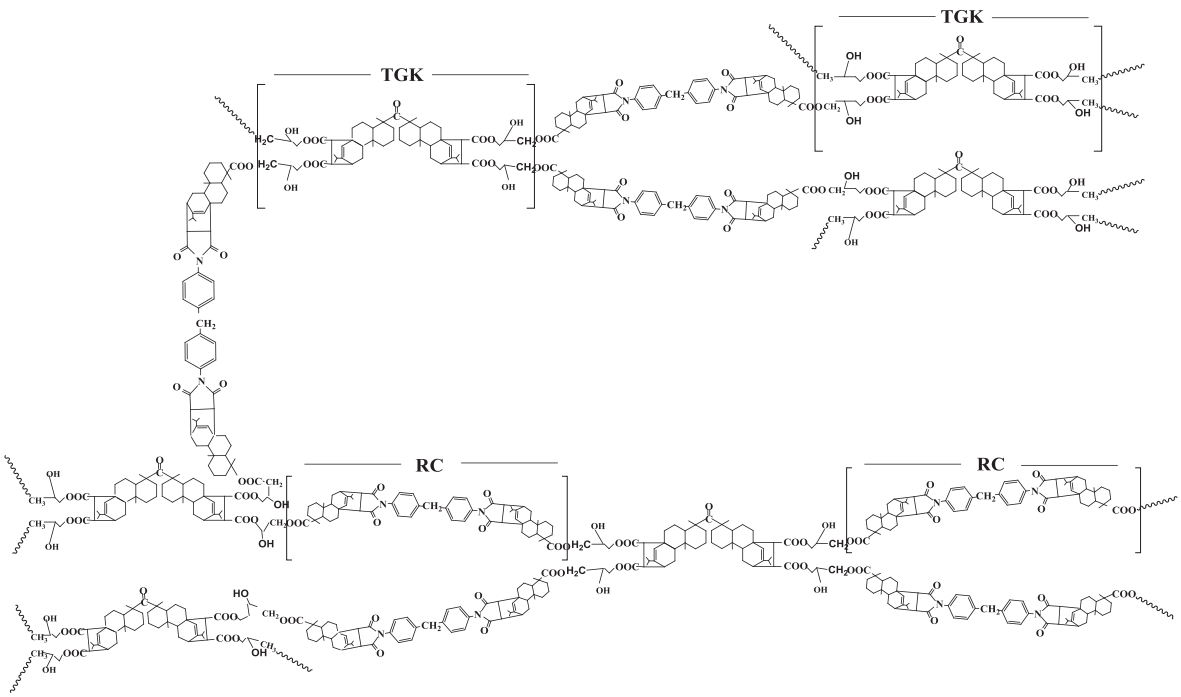

Scheme 3. Proposed crosslinked network structure for TGK/RC.

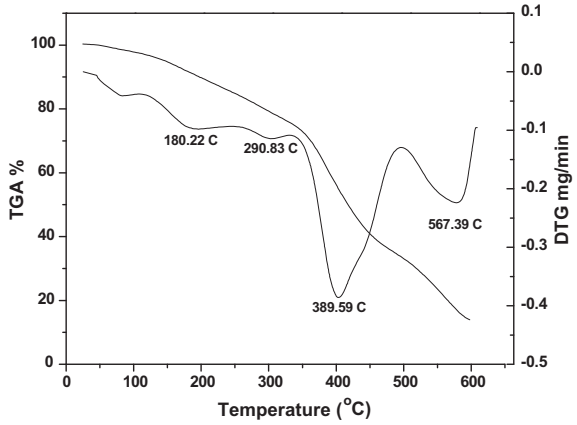

Fig. 9. TGA and DTG of cured TGK/RC epoxy system.

TGK/PPD and DGEBA/PPD, IDT was observed at 255.5 °C and 260 °C, respectively and T_{max} was 312.17 °C and 287.33 °C, respectively (see Figs. 10 and 11). Such high thermal stability may be a result of the planar structure of either phenanthrene or phenyl rings that give room for ordered packing of the rigid structures. For the same reason, it was also noted that the similarity in chemical structure of both resin and crosslinker results in better thermal stability. For comparison, Zhen et al. [18] reported the thermal stability of a ready-made epoxy resin (E-51) cured with rosin based polyamide hardener. They found that the weight loss interval was 82.99% in temperature range of 343–410.2 °C. Wu et al. [38] have evaluated the thermal stability of some epoxy resins containing flame retardant components. For neat bisphenol-A epoxy resin crosslinked with diaminodiphenylmethane (DDM), they found that IDT and T_{max} are 379 °C and 398 °C, respectively. These results are higher than that obtained by DGEBA/PPD, an observation that clearly shows that the stability of network is dependent on the type of amine used, which in turn controls the network structure. These observations shed light on the acceptable thermal stability of proposed fully rosin-based system.

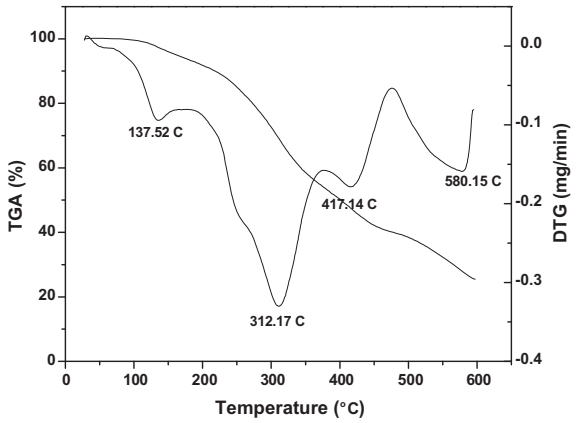

Fig. 10. TGA and DTG of cured TGK/PPD epoxy system.

3.4. DSC and POM analyses for RC

The enhancement of the storage modulus, the glass transition temperature and the thermal stability upon using RC rather than PPD, encouraged us to study the texture of the former in an attempt to detect the formation of a liquid crystal phase upon curing. The sample was heated from room temperature to 350 °C with a heating rate of 10 °C/min under nitrogen atmosphere. Two main endothermic transitions can be observed (see Fig. 12). The first transition was detected in a range of 250–370 °C while the second one was observed at 347 °C.

Polarized optical microscopy (POM) was used to investigate the formation of liquid crystal phase besides defining the obtained texture. The liquid crystals can be classified into three basic types: nematic, smectic and cholestric [39,40]. The namatic phase is the most commonly observed liquid crystalline phase [41]. Different textures of nematic liquid crystals are commonly known including: monodomain, schlieren and nematic droplet. Fig. 13(a and b) shows POM micrographs for RC obtained at 253 °C (a temperature corresponds to the range of the first transition in the DSC scan) and at 355 °C (a temperature corresponding to the end of the second transition in the DSC scan). At 253 °C (Fig. 13a) the sample appears as typical nematic droplets (NDs). Both isotropic and nematic phases can be clearly observed with the nematic droplets being surrounded by the isotropic phase. Applying director fields and polarizing microscope textures for nematic droplets reported by Kitzerow [42] and Ondris-Crawford et al. [43], the obtained NDs have a planner anchoring of the dipolar configuration. Upon increasing the temperature up to 355 °C (Fig. 13b), there is an isotropic transition for RC from the liquid crystalline phase as shown by the absence of birefringence. This agrees with Yuan et al. [44] conclusion for the possibility of crystalline (or liquid crystalline) properties of resin acid-grafted polycaprolactone.

This finding can rationalize the improvement of thermal stability and mechanical properties induced by liquid crystal crosslinkers where the rigid hydrophenanthrene exhibits excellent thermal properties by retaining the liquid–crystalline (LC) structure during the curing process. This is indeed a result of the long-range order that characterize the nematic texture experienced by the crosslinker (RC).

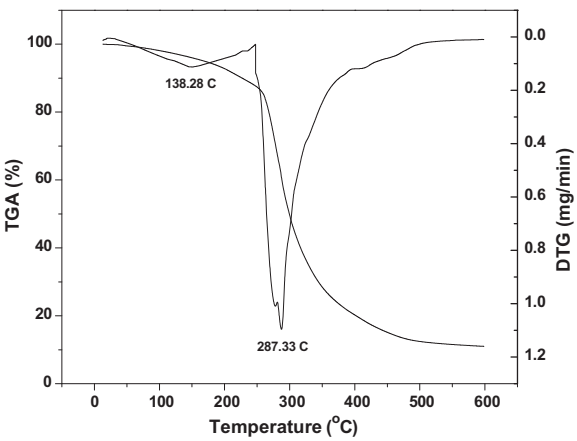

Fig. 11. TGA and DTG of cured DGEBA/PPD epoxy system.

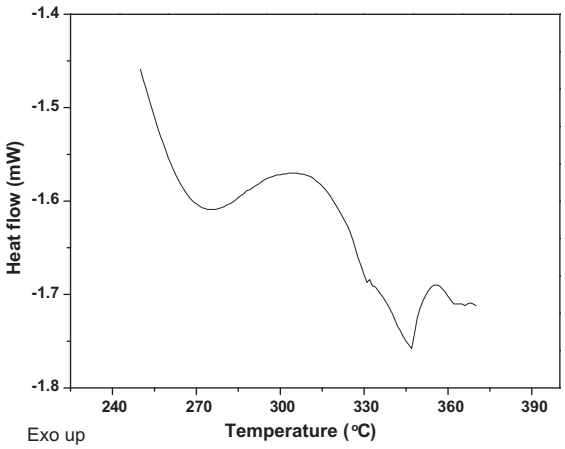

Fig. 12. DSC thermogram of RC.

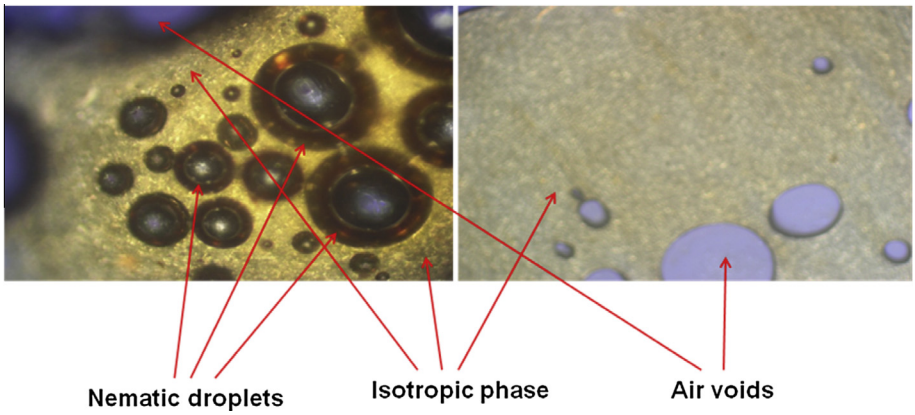

Fig. 13. POM micrographs of RC at (a) 253 °C and (b) 355 °C.

Table 3
Mechanical tests for cured epoxy resin.

Resin	Pull off resistance (MP)	Impact strength (J)	Hardness	T-bend (mm)
TGK/RC	9	8	5H	<4
TGK/PPD	6	5	2H	<4
DGEBA/PPD	4	6	4H	<4

3.5. Mechanical analyses of cured epoxy coatings

Thermosetting liquid crystalline polymers are characterized by their excellent thermal and mechanical properties [25,45]. Regarding the determined dynamic mechanical properties, the analysis is performed using free films. This is considered as a serious limitation in coating application because many, if not most, of the performance properties of coatings are influenced by coating-substrate interactions. Therefore, tests of coatings intact on their end-use substrates must be thoughtfully coupled with free film determinations. Thus dynamic mechanical analysis (DMA) would be useful when interpreted coupled with results of adhesion, abrasion, hardness and others. Results of pull-off (in MP), impact strength (in Joules), hardness grade and bending are presented in Table 3. Higher pull-off resistance (adhesion strength) was achieved by both TGK/RC and TGK/PPD than that of DGEBA/PPD. Moreover, good adherence and flexibility of coating systems were observed during the bending tests (Table 3). This can be attributed to the strong interaction of multiple polar moieties like ester, imide and carbonyl of either TGK resin or crosslinker with the substrate. The high impact strength and hardness attained by TGK/RC and DGEBA/PPD (Table 3) reflect the optimum crosslinking. Such results support using TGK/RC coat for high performance industrial applications.

4. Conclusions

Rosin acid based tetra-functional epoxy (TGK) and thermotropic liquid crystal crosslinker (RC) with nematic droplets texture were successfully prepared. Viscoelastic properties and thermal stability of the fully bio-based epoxy system were compared with those containing commercial bisphenol-A epoxy (DGEBA) and/or p-phenylene diamine (PPD) crosslinker. Storage modulus for the cured TGK/RC sample was found to be comparable to DGEBA/PPD while glass transition temperature of the former is 50 °C higher. Incorporation of rosin acid into epoxy architecture levels up temperatures of initial and maximum degradation. Mechanical testing of coated steel panels proved that rosin based epoxy is suitable for coating application.

Acknowledgement

This project was supported financially by the Science and Technology Development Fund (STDF), Egypt, Grant No. 4225.

References

[1] J. Soltes, D.F. Zinkel, Chemistry of rosin, in: D.F. Zinkel, J. Russel (Eds.), Naval Stores. Production, Chemistry, Utilization, Pulp Chemical Association, New York, 1989, pp. 261–345.
[2] M. Rizzo, G. Bruno, Surface Coatings: Volume 1, Raw Materials and Their Usage, in: Science, Oil and Colour Chemists' Association, Springer Science and Business Media, 1993, pp. 149–150.
[3] J.J.W. Coppen, G.A. Hone, Gum Naval Stores: Turpentine and Rosin From Pine Resin, Natural Resources Institute, Food and Agriculture Organization of the United Nations, Rome, 1995.
[4] F. Mustata, I. Bicu, Hydroxyesters of resin acids modified with o-cresol/p-nonylphenol/formaldehyde resins, Polymery 54 (9) (2009) 627–634.
[5] D.W. Kang, D.K. Yoon, S.H. Ji, Synthesis and characterization of rosinester modified with p-nonylphenolic resole, J. Ind. Eng. Chem. 6 (4) (2000) 256–261.
[6] Y.B. Ha, M.Y. Jin, S.S. Oh, D.H. Ryu, Synthesis of an environmentally friendly phenol-free resin for printing ink, Bull. Kor. Chem. Soc. 33 (10) (2012) 3413–3416.
[7] J. Yu, N. Xu, Z. Liu, L. Wang, Novel one-component positive-tone chemically amplified i-line molecular glass photoresists, ACS Appl. Mater. Interfaces 4 (5) (2012) 2591–2596.
[8] I. Bicu, F. Mustata, Ketone derivatives of Diels–Alder adducts of levopimaric acid with acrylic acid and maleic anhydride: synthesis, characterization and polymerization, J. Appl. Polym. Sci. 92 (4) (2004) 2240–2252.
[9] I. Bicu, F. Mustata, Polymers from a levopimaric acid–acrylic acid Diels–Alder adduct: Synthesis and characterization, J. Polym. Sci., Part A: Polym. Chem. 45 (24) (2007) 5979–5990.
[10] F. Mustata, I. Bicu, A novel route for synthesizing esters and polyesters from the Diels–Alder adduct of levopimaric acid and acrylic acid, Eur. Polym. J. 46 (6) (2010) 1316–1327.
[11] X. Liu, C. Li, G. Guan, X. Yuan, Y. Xiao, D. Zhang, Crystallization behavior and morphology of poly(butylene succinate) modified with rosin maleopimaric acid anhydride, J. Polym. Sci., Part B: Polym. Phys. 43 (19) (2005) 2694–2704.
[12] X.Q. Liu, W. Huang, Y.H. Jiang, J. Zhu, C.Z. Zhang, Preparation of a bio-based epoxy with comparable properties to those of petroleum-based counterparts, Exp. Polym. Lett. 6 (4) (2012) 293–298.
[13] J. Wang, C. Wang, C. Tang, F. Chu, Preparation and characterization of rosin-based polymeric monomer, in: Proceeding of the 55th International Convention of Society of Wood Science and Technology, August 27–31, Beijing, China, 2012.
[14] X. Liu, J. Zhang, High-performance biobased epoxy derived from rosin, Polym. Int. 59 (5) (2010) 607–609.
[15] C. Mantzaridis, A.-L. Brocas, A. Llevot, G. Cendejas, R. Auvergne, S. Caillol, S. Carlotti, H. Cramail, Rosin acid oligomers as precursors of DGEBA-free epoxy resins, Green Chem. 15 (11) (2013) 3091–3098.
[16] X. Liu, W. Xin, J. Zhang, Rosin-derived imide–diacids as epoxy curing agents for enhanced performance, Bioresour. Technol. 101 (7) (2010) 2520–2524.
[17] H. Wang, B. Liu, X. Liu, J. Zhang, M. Xian, Synthesis of biobased epoxy and curing agents using rosin and the study of cure reactions, Green Chem. 10 (2008) 1190–1196.
[18] M.I. Zhen, N.I.E. Xiao-an, W. Yi-gang, C. Xia, L.I.N. Gui-fu, Study on synthesis and performance of rosin-derived polyamide as epoxy curing agent, J. For. Prod. Ind. 2 (2) (2013) 5–11.
[19] H. Wang, X. Liu, B. Liu, J. Zhang, M. Xian, Synthesis of rosin-based flexible anhydride-type curing agents and properties of the cured epoxy, Polym. Int. 58 (12) (2009) 1435–1441.
[20] X. Liu, W. Xin, J. Zhang, Rosin-based anhydrides as alternatives to petrochemical curing agents, Green Chem. 11 (2009) 1018–1025.
[21] F. Jaillet, E. Darroman, A. Ratsimihety, R. Auvergne, B. Boutevin, S. Caillol, New biobased epoxy materials from cardanol, Eur. J. Lipid Sci. Technol. 116 (1) (2014) 63–73.
[22] I. Bicu, F. Mustata, Crosslinked polymers from resin acids, Angew. Makromol. Chem. 234 (1) (1996) 91–102.
[23] I. Bicu, F. Mustata, Study of the condensation products of abietic acid with formaldehyde at high temperatures, Angew. Makromol. Chem. 222 (1) (1994) 165–174.
[24] X. Liu, C. Li, D. Zhang, Y. Xiao, G. Guan, Synthesis, characterization and properties of poly(butylene succinate) modified with rosin maleopimaric acid anhydride, Polym. Int. 55 (5) (2006) 545–551.
[25] D. Gulino, J. Galy, J.P. Pascault, Etude des prépolymères époxydes par chromatographie et ^{1}H NMR a′ 350 MHz, Makromol. Chem. 184 (2) (1983) 411–429.
[26] W.-F.A. Su, K.C. Chen, S.Y. Tseng, Effects of chemical structure changes on thermal, mechanical, and crystalline properties of rigid rod epoxy resins, J. Appl. Polym. Sci. 78 (2) (2000) 446–451.
[27] A.-L. Brocas, A. Llevot, C. Mantzaridis, G. Cendejas, R. Auvergne, S. Caillol, S. Carlotti, H. Cramail, Epoxidized rosin acids as co-precursors for epoxy resins, Des. Monomers Polym. 17 (4) (2014) 301–310.
[28] Q.-H. Zhou, M. Li, P. Yang, Y. Gu, Effect of hydrogen bonds on structures and glass transition temperatures of maleimide–isobutene alternating copolymers: molecular dynamics simulation study, Macromol. Theory Simul. 22 (2) (2013) 107–114.
[29] L.H. Sperling, Introduction to Physical Polymer Science, 4th ed., Wiley, Hoboken, NJ, USA, 2005.
[30] W.-F.A. Su, K.C. Chen, S.Y. Tseng, Effects of chemical structure changes on thermal, mechanical, and crystalline properties of rigid rod epoxy resins, J. Appl. Polym. Sci. 78 (2) (2000) 446–451.
[31] J.Y. Lee, J. Jang, S.S. Hwang, S.M. Hong, K.U. Kim, Synthesis and curing of liquid crystalline epoxy resins based on 4,4′-biphenol, Polymer 39 (24) (1998) 6121–6126.
[32] J.A. Mikroyannidis, Self-curing epoxy compounds, J. Appl. Polym. Sci. 41 (11–12) (1990) 2613–2624.
[33] M. Ochi, Y. Shimizu, Y. Nakanishi, Y. Murata, Effect of the network structure on thermal and mechanical properties of mesogenic epoxy resin cured with aromatic amine, J. Polym. Sci., Part B: Polym. Phys. 35 (2) (1997) 397–405.

[34] F. Fraga, E.R. Nunez, Activation energies for the epoxy system BADGE n = 0/m-XDA obtained using data from thermogravimetric analysis, J. Appl. Polym. Sci. 80 (5) (2001) 776–782.
[35] F. Fraga, E.R. Nunez, Master curves and lifetime prediction for the epoxy system badge n = 0/m-XDA by thermogravimetric analysis, J. Appl. Polym. Sci. 82 (2) (2001) 461–466.
[36] F. Fraga, E.R. Nunez, Lifetime predictions for the epoxy system BADGE n = 0/m-XDA using kinetic analysis of thermogravimetry curves, J. Appl. Polym. Sci. 83 (8) (2002) 1692–1696.
[37] L. Barral, J. Cano, J. López, J. López-Bueno, P. Nogueira, C. Ramírez, M.J. Abad, Degradation kinetics of an epoxy/cycloaliphatic amine resin under isothermal and non-isothermal conditions, J. Therm. Anal. Calorim. 55 (1) (1999) 37–45.
[38] C.S. Wu, Y.L. Liu, Y.C. Chiu, Y.S. Chiu, Thermal stability of epoxy resins containing flame retardant components: an evaluation with thermogravimetric analysis, Polym. Degrad. Stab. 78 (1) (2002) 41–48.
[39] D. Demus, G. Pelzl, R. Zentel, Topics in physical chemistry, in: H. Baumgärtel, E.U. Franck, W. Grünbein, H. Stegemeyer (Eds.), Liquid Crystals, vol. 3, Steinkopff Darmstadt Springer, New York, 1994 (Ch. 1–3).
[40] G.W. Gray, P.A. Winsor, A. Saupe, H. Zocher, P.G. de Gennes, M. Kléman, in: G.W. Gray, P.A. Winsor (Eds.), Liquid Crystals & Plastics Crystals, vol. 1, John Wiley & Sons, New York, 1974 (Ch. 1–3).
[41] T.-S. Chung, S.-X. Cheng, M. Jaffe, in: Tai-Shung Chung (Ed.), Thermotropic Liquid Crystal Polymers: Thin-Film Polymerization, Characterization, Blends, and Applications, Technomic Publishing Company, Inc., Lancaster, Pennsylvania – USA, 2001 (Ch. 1).
[42] H-S. Kitzerow, Polymer-dispersed liquid crystals from the nematic curvilinear aligned phase to ferroelectric films, Liq. Cryst. 16 (1) (1994) 1–31.
[43] R. Ondris-Crawford, E.P. Boyko, B.G. Wagner, J.H. Erdmann, S. Zumer, J.W. Doane, Microscope textures of nematic droplets in polymer dispersed liquid crystals, J. Appl. Phys. 69 (9) (1991) 6380–6386.
[44] L. Yuan, N. Hamidi, S. Smith, F. Clemons, A. Hamidi, C. Tang, Molecular characterization of biodegradable natural resin acid-substituted polycaprolactone, Eur. Polym. J. 62 (2015) 43–50.
[45] C. Carfagna, G. Meo, L. Nicolais, M. Giamberini, A. Priola, G. Malucelli, Composites based on carbon fibers and liquid crystalline epoxy resins, 2 Dynamic-mechanical analysis and fracture toughness behavior, Macromol. Chem. Phys. 201 (18) (2000) 2639–2645.